ORIGINAL ARTICLE



Thermal, mechanical, and morphological studies of a depolymerizable graft copolymer thermoplastic

Zeyu Wang¹ · Mark D. Foster¹ · Junpeng Wang¹

Received: 20 May 2023 / Revised: 29 June 2023 / Accepted: 17 July 2023 / Published online: 3 August 2023 © The Society of Polymer Science, Japan 2023

Abstract

Graft polymers are gaining increasing interest because of their unique architectural characteristics. We recently reported a novel type of depolymerizable graft polymer based on poly(*trans*-cyclobutane fused cyclooctene), in an effort to address the trade-off between depolymerizability and controlled grafting-through polymerization. In this work, we examine the thermal, mechanical, and morphological properties of a graft copolymer thermoplastic material prepared by copolymerizing poly(L-lactide) and margaric acid-based macromonomers. A copolymerization kinetics study reveals that the two macromonomers are incorporated almost randomly and that the domain spacing measured from small-angle X-ray scattering is consistent with the random distribution. An investigation of the crystallization behavior suggests that proper thermal treatment is required to maximize, or to even observe crystallinity. The physical states of the soft and hard domains, whether melt, glassy, or semicrystalline, significantly impact the tensile properties of the resulting copolymer materials. Finally, the rheological properties and morphological features are discussed.

Introduction

Graft polymers have been proven to be superior polymeric building blocks in various applications, such as thermoplastic elastomers [1–3], tissue-mimicking soft elastomers [4–8], and photonic crystals [9–11]. The high structural complexity in graft polymers' architectures, relative to linear polymers, enables access to a wider array of material properties. From the structural perspective, regardless of the constituents, a linear polymer can be simply described by a single degree of polymerization (DP), whereas description of a graft polymer requires four parameters: degree of polymerization of the backbone ($DP_{\rm bb}$), degree of polymerization of the side chains ($DP_{\rm sc}$), degree of

Supplementary information The online version contains supplementary material available at https://doi.org/10.1038/s41428-023-00826-0.

- Mark D. Foster mdf1@uakron.edu
- School of Polymer Science and Polymer Engineering, University of Akron, Akron, OH 44325, USA

polymerization between adjacent side chains (DP_g), and a description of the manner in which the grafts are distributed along the backbone (e.g., randomly spaced or with all pairs of adjacent grafts separated by the same spacing). Varying these structural parameters can greatly influence the material properties, including tensile behavior [2, 3, 8, 12], rheological response [13–15], and thermal behavior [14, 16–18].

It is possible to leverage the architectural advantages of graft polymers to access both high molecular weight (robust properties) and low viscosity (easy processing). However, good control over the molecular weights and structures of graft polymers is necessary to achieve the desired properties. Among the three common grafting methods, namely grafting-through, grafting-to, and grafting-from, the grafting-through approach is the most versatile due to its precise control over the molecular weight, grafting density, and backbone and side chain compositions. Ring-opening metathesis polymerization (ROMP) of norbornene-derived monomers is one of the most commonly used methods for obtaining graft polymers, due to its high reactivity under mild conditions and excellent tolerance to functional groups. However, the highly exergonic nature ($\Delta G \ll 0$) required for the grafting-through polymerization of macromonomers renders the resulting polymers non-depolymerizable, prohibiting the sustainable use of these materials.

We recently reported grafting-through ROMP of transcyclobutane fused trans-cyclooctene (tCBtCO) macromonomers and the subsequent depolymerization into the cis-cyclooctene counterparts (tCBcCO) [19]. The isomerization from cis- to trans-alkene in the eight-membered ring elevates the ring strain and thus the driving force for the polymerization, allowing for controlled polymerization. The resulting graft polymers, in the presence of an olefin metathesis catalyst, can be depolymerized to the thermodynamically favored cis-cyclooctene isomers. We also demonstrated a ductile thermoplastic material synthesized from statistical copolymerization of a monomer containing a poly(L-lactide) (PLLA) side chain and a monomer containing a margaric acid (MA) side chain. In this work, we focus on the thermal, mechanical, and morphological characterizations of this chemically recyclable thermoplastic, providing insights into the design of next-generation sustainable materials.

Materials and methods

Materials

The graft polymers, P1-stat-P2, P1-stat-P3, P1, P2 and P3, studied in this work were synthesized according to methods described in our previous report [19]. The graft copolymer with margaric acid side chains referred to as "P1-stat-P2" herein is denoted as "P1-stat-P3" in ref. 19. The graft polymer referred to as "P1-stat-P3" herein has stearic acid (SA)-containing side chains and is new to this work.

Nuclear magnetic resonance (NMR) spectroscopy

 1 H spectra were obtained at the University of Akron Magnetic Resonance Center using a Varian NMR 500 MHz spectrometer. Chemical shifts (δ) were reported in parts per million (ppm), referenced to the residual nondeuterated chloroform peak ($\delta = 7.26$ [1 H]). The NMR spectra were obtained and analyzed using Agilent VnmrJ and MestRe-Nova software, respectively. The NMR spectra for **3** and **P1-stat-P3** are shown in Supplementary Figs. S1 and S2, respectively.

Size-exclusion chromatography (SEC)

SEC was performed on a Tosoh EcoSEC HLC-8320GPC with two TSKgel GMHHR-M(S) analytical columns (7.8 mm inner diameter \times 30 cm, 13 μ m) and one TSKgel guard column H_{HR}(S) (7.5 mm inner diameter \times 7.5 cm, 13 μ m), connected in series with a built-in refractive index (RI) detector and a miniDAWN TREOS multi-angle light

scattering (MALS) detector (Wyatt Technology). Experiments were run at 40 °C at a flow rate of 1 mL/min in THF.

Differential scanning calorimetry (DSC)

DSC was performed on a TA Discovery DSC 250 using hermetic aluminum pans under a nitrogen atmosphere. The results were processed with TA TRIOS software.

Small-angle X-ray scattering (SAXS)

SAXS measurements were conducted at the Advanced Materials and Liquid Crystal Institute at Kent State University on a Xeuss 3.0 apparatus in transmission mode. The circular collimation apertures had diameters of 1.2 mm and 0.7 mm. The sample-to-detector distance was 900 mm. The beam, which was obtained from a CuK_α microfocus source, had a wavelength of 1.54 Å. The SAXS sample was prepared as follows. The polymer was dissolved in dichloromethane and filtered through a PTFE syringe filter (pore size 0.22 µm) into a PTFE beaker to obtain a film upon drying in a vacuum oven. About 7 mg of the sample was placed in an aluminum washer (inner diameter: 4 mm, thickness: 0.6 mm) using a spatula. The sample-filled washer was covered with PTFE films on both sides, sandwiched between two glass slides, and fixed with binder clips. The whole assembly was placed in an oven at 170 °C for 3 h for sample molding and annealing. The washer containing the polymer was taped with Mylar films on both sides to provide cell windows with high X-ray transmission.

Rheology

A TA Discovery HR-2 rotational rheometer with an 8 mm diameter parallel plate geometry was used for rheological measurements. The sample was loaded and softened at elevated temperature to give an approximately 1-mm gap between plates. A dynamic strain sweep was conducted first to define the range of strain for linear viscoelastic response, and a strain of 1% was chosen for all subsequent experiments. Frequency sweeps were carried out at various temperatures in the melt state over an experimentally convenient frequency range of 0.1–100 rad/s.

Tensile testing

Uniaxial tensile testing (ASTM D1708-18) was performed at a crosshead velocity of 5 mm/min on an Instron 5543 universal testing machine equipped with a 100 N load cell using a gripping pressure of 25 psi on the pneumatic grips. Dumbbell specimens (ASTM D 638 Type IV) were prepared by compression molding in a steel mold sandwiched

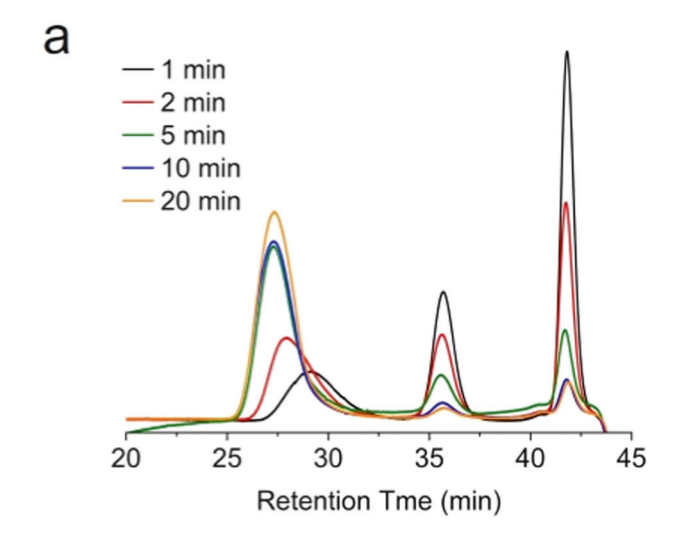
between PTFE sheets under 5000 lbf at 170 °C for 3 min using a hydraulic Carver Press.

Results and discussion

Following our previous report [19], the depolymerizable graft copolymer was synthesized by copolymerization of 1 and 2 in the presence of Grubbs first-generation catalyst (G1) and triphenylphosphine (PPh₃). A [1]₀/[2]₀/[G1]/ [PPh₃] ratio of 300/2700/1/30 was used (Fig. 1). The resulting copolymer was characterized using ¹H NMR spectroscopy to have a **P1**-to-**P2** mass ratio of 1.1:1. The M_n of P1-stat-P2 was determined using SEC-RI/MALS to be 2800 kDa, and a dispersity (D) of 1.10 was obtained (SI for ref. 19). For P1-stat-P3 (NMR spectrum in Supplementary Fig. S2), the **P1**-to-**P3** mass ratio was 1:1. The M_n of **P1**stat-P3 was determined to be 1700 kDa, with D = 1.02(Supplementary Fig. S3). It has been shown that the feed ratio and sizes of the (macro)monomers could greatly influence the reactivity ratio and therefore the side chain distribution along the backbone [20], possibly leading to variations in the material performance. For a thermoplastic consisting of hard and soft domains formed by microphase separation, random incorporation would be desired to ensure robust physical crosslinking. Thus, to understand the microstructure of our copolymer, we measured the copolymerization kinetics using SEC-RI by monitoring the evolution of the peak areas of the monomers and polymer (Fig. 2a). Despite the large difference in the sizes of monomers 1 and 2, they were consumed at similar rates (mass per time) over the course of 20 min and up to conversions of 92% and 93% for 1 and 2, respectively (Fig. 2b); this result indicated that the distribution of side chains along the backbone length was nearly random and nearly uniform from one end of the backbone to the other.

The thermal properties of a thermoplastic material are of great importance in determining the optimal processing conditions, such as temperature and duration. Differential scanning calorimetry (DSC) thermograms of **P1-stat-P2** revealed only one exotherm at $-1.8\,^{\circ}\text{C}$ and one endotherm at $12.2\,^{\circ}\text{C}$ in the first cooling and second heating cycles (Fig. 3a), respectively. These two features, both well below room temperature, correspond to the crystallization and

melting of the MA side chains, respectively. These observations suggested that the PLLA segments tethered to the graft polymer backbone were not able to crystallize when cooled from the melt at a rate of 1 °C/min or when heated from the glassy state at a rate of 10 °C/min. The large spacing between two PLLA grafts (79 C-C bonds on



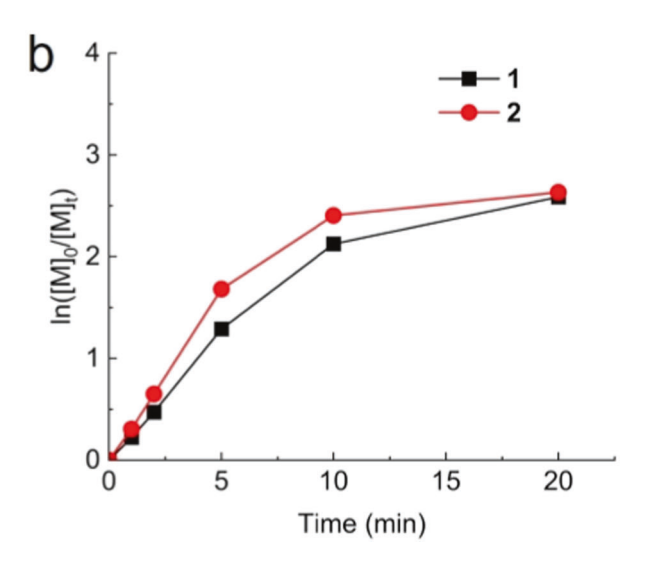
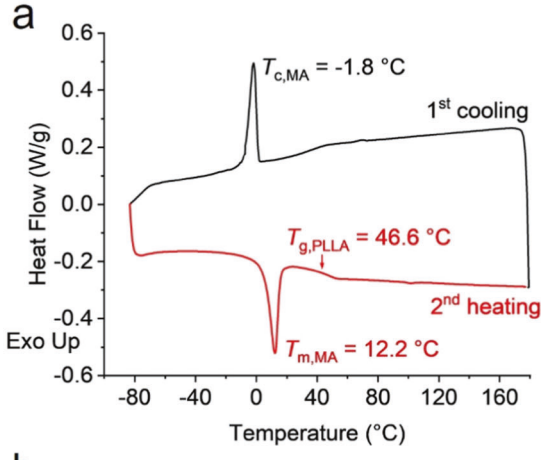
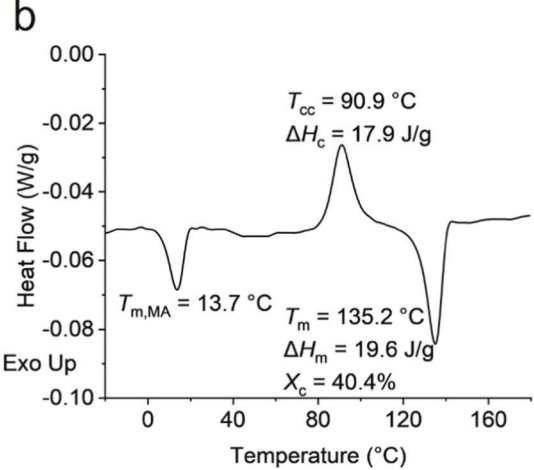


Fig. 2 Kinetics of the copolymerization of 1 and 2 in the presence of G1 and PPh3. (a) Evolution of SEC traces over ROMP time and (b) dependence of logarithmic conversions $\ln([M]_0/[M]_t)$ of 1 and 2 over time

Fig. 1 Synthesis of the graft copolymers P1-stat-P2 and P1-stat-P3 by ring-opening metathesis copolymerization





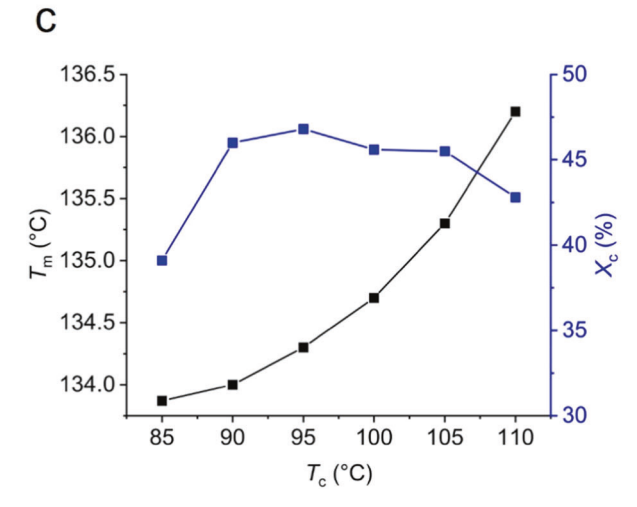


Fig. 3 DSC thermograms of P1-stat-P2. a Cooling curve at 1 °C/min (black) following a first heating to remove thermal history and a second heating curve at 10 °C/min (red). b Second heating curve at a slower rate of 1 °C/min after melt-quenching (rather than slow cooling) from 180 °C, showing melting peaks for both microdomains rich in MA side chains and microdomains rich in PLLA side chains. c Dependence of the melting temperature of PLLA side chain-rich regions, $T_{\rm m}$, and the percent crystallinity, $X_{\rm c}$, on the isothermal crystallization temperature, $T_{\rm c}$

average) and the low mobility due to the large overall M_n likely frustrated the crystalline packing of the PLLA grafts. In contrast, the DSC thermogram of the graft copolymer with only PLLA side chains, P1, (Supplementary Fig. S4) exhibited two endothermic peaks on the second heating ramp corresponding to the crystallization of PLLA side chains. The second peak was due to melting of the crystals resulting from recrystallization of defective crystals created first as a result of the limited mobility of the brush PLLA side chains [21]. The T_c and T_m values of the MA side chains were lower in the copolymer (-1.8 and 12.2 °C, respectively, Fig. 2a) than those in the homopolymer P2 (1.9 and 19.8 °C, respectively; Supplementary Fig. S5), also indicating the frustration of side chain packing for a copolymer with two different graft components [22]. The presence of a melting peak for MA side chains of P1-stat-P2 at a temperature below the glass transition of PLLA (44 °C) in Fig. 3b indicated the presence of two types of microdomains rich in side chains, one rich in MA side chains $(T_{\rm m, MA})$ and the other rich in PLLA side chains.

By changing the first cooling to a rapid melt quench from 180 °C and reducing the heating rate to 1 °C/min for the second heating curve, upon heating, cold crystallization $(T_{cc} = 90.9 \,^{\circ}\text{C})$ and subsequent melting $(T_{m} = 135.2 \,^{\circ}\text{C})$ were clearly observed (Fig. 3b); the calculated crystallinity (X_c) of PLLA was 40.4%, based on a specific enthalpy of fusion of $\Delta H_f^0 = 93 \text{ J/g}$ for PLLA [23]. The results encouraged us to determine whether we could maximize the PLLA side chain crystallinity by finding the optimal crystallization temperature. Isothermal crystallizations from the melt-quenched glassy state were performed at various annealing temperatures below T_c, spanning from 85 to 110 °C. After 180 min of annealing, the sample was cooled at 10 °C/min to -90 °C, and then heated at 5 °C/min to reveal the melting endotherms (Supplementary Fig. S6). $T_{\rm m}$ increased monotonically with $T_{\rm c}$ over this range of $T_{\rm c}$, and a maximum X_c value of 47% was found for an annealing temperature of 95 °C (Fig. 3c).

As shown in the recent work by Hillmyer et al., switching from amorphous PLA to semicrystalline PLLA as the side chain to form physical crosslinking domains in graft copolymer thermoplastic elastomers significantly improves the mechanical properties [2]. To investigate the role crystallinity plays in the mechanical behavior of our system, we compared the tensile properties of amorphous and semicrystalline **P1-stat-P2** samples. The as-molded **P1-stat-P2** was determined to be amorphous according to DSC, which was consistent with the absence of melt crystallization of PLLA side chains, as shown in Fig. 3a. To obtain semicrystalline **P1-stat-P2**, the tensile bar was annealed at 95 °C in an oven for 3 h. A DSC scan confirmed a PLLA crystallinity of 50.0% after annealing (Supplementary Fig. S7). The annealed sample was much more ductile than

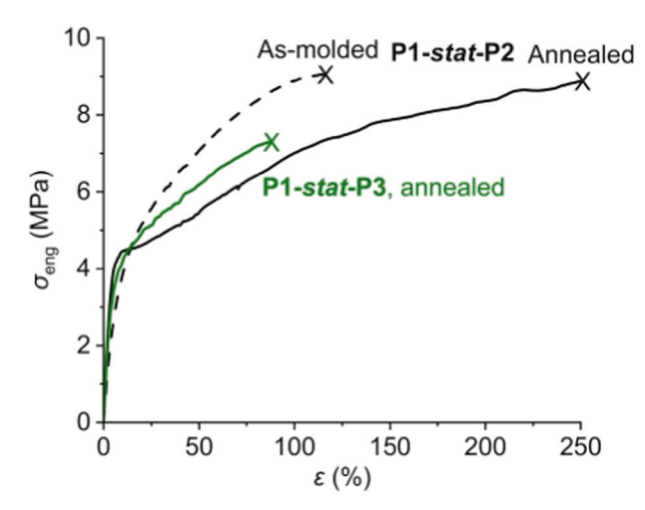


Fig. 4 Tensile stress-strain curves of the graft copolymers

was the as-molded sample (Fig. 4), demonstrating the importance of crystallinity in enhancing the material performance.

Notably, the state of the fatty acid soft domain played an important role in determining the mechanical properties of the graft copolymers. Although the alkyl side chain could densely pack into crystalline domains, as evidenced by DSC (Fig. 3b), the $T_{\rm m,MA}$ (13.7 °C) was lower than the ambient temperature, suggesting the presence of melted MA side chain-rich microdomains at room temperature. However, when we introduced SA as the side chain instead of MA to yield P1-stat-P3, the SA side chains formed a crystalline phase that could persist for sufficiently low room temperature ($T_{m,SA} = 25.2$ °C, Fig. S8). The annealed **P1-stat-**P3 was significantly weaker and less ductile than both the as-molded and annealed P1-stat-P2 (Fig. 4). This phenomenon was indicative of the importance of having both soft and hard domains in achieving ductility in thermoplastic materials. The tensile properties of the graft copolymers studied in this work are summarized in Table 1.

To understand the viscoelastic properties of the thermoplastic **P1-stat-P2**, small-amplitude oscillatory shear (SAOS) experiments were carried out above the melting temperature of PLLA. In the low-frequency regime at a temperature of 180 °C, the material exhibited nonliquid-like scaling $(G' \sim \omega, G'' \sim \omega^{0.8})$ (Fig. 5a), indicating a microphase-separated structure [3, 12]. As shown in Fig. 5b, the graft copolymer possessed relatively low complex viscosity (10^2-10^4Pa·s) around the molding temperature of 170 °C, despite having a very large $M_{\rm w}$ (3700 kDa), due to the barely entangled structure. A shear-thinning response was exhibited at all temperatures for which measurements were performed, potentially facilitating the material's processability. The absence of a frequency-independent zero-shear viscosity at a low

Table 1 Summary of the tensile properties of the graft copolymers

Sample	E (MPa)	ε _b (%)	σ _b (MPa)
P1-stat-P2	120	260	8.9
P1-stat-P2, as-molded	71	120	9.1
P1-stat-P3	99	87	7.3

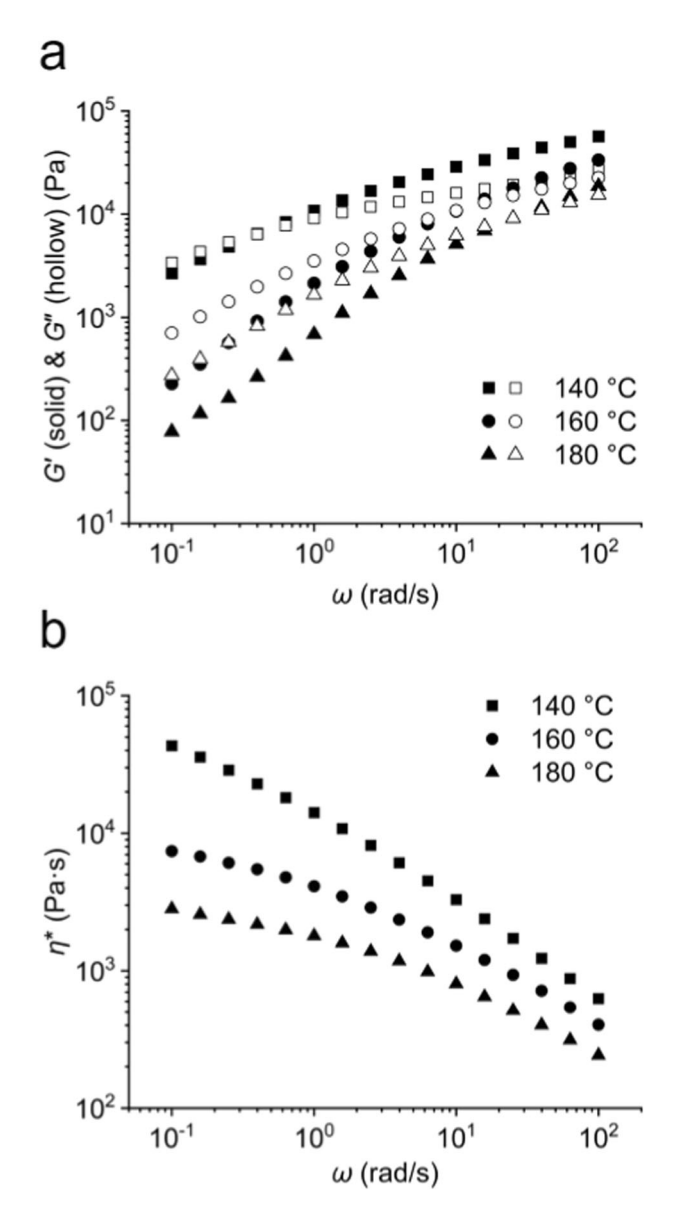


Fig. 5 Rheological properties of P1-stat-P2: (a) dynamic shear moduli and (b) complex viscosity frequency sweep at various temperatures

frequency across all temperatures tested further aligned with the premise of a microscopic phase-separated structure.

X-ray scattering measurements were employed to gain insights into the morphological features of the **P1-stat-P2** samples. Our previous small-angle X-ray scattering (SAXS) measurement of an as-molded sample revealed a single broad principal peak, suggesting microphase separation and

a poorly ordered morphology. The calculated domain spacing $(d = 2\pi/q^*)$ of 17 nm was close to that of a previously reported brush random copolymer (d = 14 nm) comprising PLLA sidechains with graft length comparable to that of our sample [24], further supporting the random incorporation of 1 and 2 (as discussed in the polymerization kinetics section). Because the soft and hard domains were comparable in volume, such a material was likely to form a cocontinuous morphology similar to that of segmented polyurethane [25]. Despite the crystallizable PLLA side chains, there was no Bragg peak but only an amorphous halo in the wide-angle X-ray scattering (WAXS) pattern (Fig. 6a) in the as-molded sample, which was consistent with the absence of melt crystallization observed in DSC in Fig. 3a. Crystallization of the PLLA side chains was not required for microphase separation, but the degree of crystallization would affect the morphology of microphase separation. Changes in the morphology caused by side chain crystallization were surveyed quickly with a few measurements at different temperatures. As mentioned above, 95 °C was an optimal annealing temperature for crystallizing PLLA side chains in the graft copolymer. Therefore, the sample temperature was increased rapidly from 23 °C to 95 °C and held for 5 min before collecting data over 3 min as the PLLA side chains began to crystallize. Even with only approximately 12% PLLA crystallinity, the scattering pattern was significantly changed. First, two distinct peaks appeared in the WAXS region (q = 1.16 and 1.33 Å^{-1}), corresponding to the $(110)/(200)\alpha/\alpha'$ and $(203)\alpha/\alpha'$ peaks, respectively, as observed by Heeley et al. [26] for crystalline PLLA with a mixture of α and α' crystal forms. In addition, the principal peak dramatically changed shape, presumably due to the growth of a second population of domain spacings associated with the developing crystalline regions. The predominant principal peak in the SAXS region shifted slightly to the right (from 0.0365 to 0.0389 Å^{-1} , Fig. 6b), indicating a small reduction in domain spacing associated nominally with amorphous PLLA-rich microdomains. At the same time, a substantial shoulder appeared on the low q side of the principal peak, suggesting the presence of a second distribution of larger domain spacings, presumably due to PLLA side chains stretching even further from the backbone with crystallization. A peak of medium strength observed at approximately 0.18 Å⁻¹ at 23 °C was still present at 95 °C but was decidedly weaker. We surmise that this peak was not associated with the microphase segregation of the PLLA-rich domains, because it was nearly unchanged with heating from 95 °C to 170 °C over 5 min and then annealing at 170 °C for 5 min.

This further heating to 170 °C led to the melting of the PLLA crystalline regions, as evidenced by the disappearance of the corresponding peaks in the WAXS region. When the PLLA side chains melted, the principal

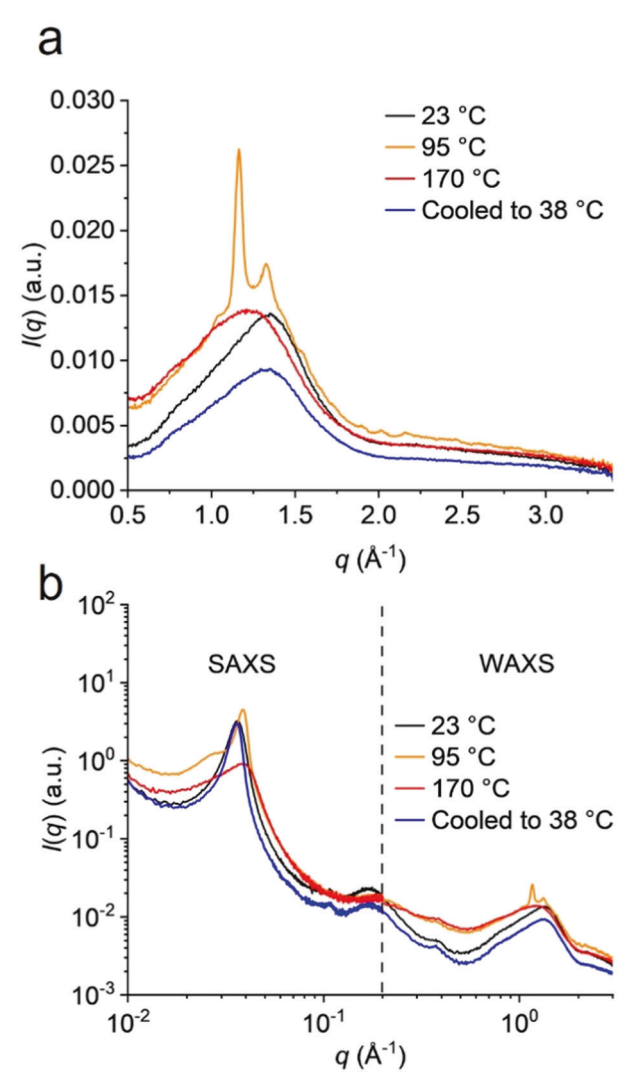


Fig. 6 (a) WAXS profiles and (b) combined SAXS and WAXS curves of **P1-stat-P2** measured at different temperatures as marked. The curve marked 95 °C was measured after heating the sample to 95 °C and holding the temperature for 5 min. The curve marked 170 °C was measured after heating further and holding the temperature at 170 °C for 5 min

peak again strongly changed shape. The shoulder disappeared, and the reestablished single peak broadened and shifted to a higher q than before, suggesting that the microphase separation of the PLLA-rich domains had substantially weakened. Determining whether the morphological signature of an order-disorder transition for those regions was passed as the temperature increased to $170\,^{\circ}\text{C}$ will require future detailed study of the changes in peak shape and intensity with temperature. When the sample was subsequently allowed to cool in vacuum to $38\,^{\circ}\text{C}$ over approximately two hours, the PLLA side chains did not recrystallize, consistent with the observation that they did not crystallize readily from the melt.

As already noted, the peak at $0.18 \,\text{Å}^{-1}$ was not related directly to the PLLA-rich microdomains. Instead, we

propose that this peak was related to the microdomains rich in aliphatic side chains. If so, this peak position corresponds to a domain spacing of approximately 3.5 nm. The fully extended length of MA is 2.24 nm, and taking the linker into account, the fully extended length of the size chain would be about 3 nm. Since these side chains are not crystalline at room temperature, they are not fully extended, and there may also be sufficient space between neighboring aliphatic side chains for some interdigitation of side chains from adjacent backbones, so such a domain spacing is reasonable. With an increase in temperature to 95 °C, this peak nearly disappeared, suggesting that the aliphatic side chains were no longer microphase separated and that the weak peak remaining was from correlation hole scattering due to the fact that the side chains were attached to the backbone.

Two additional features in the X-ray scattering deserve remark. The first is a weak peak appearing at approximately $0.107~{\rm \AA}^{-1}$ that disappeared upon increasing the temperature to 95 °C and reappeared upon subsequent cooling to 38 °C. The significance of this peak remains under investigation.

The last feature was seen near 0.4 Å⁻¹ in all of the curves. The peak position was close to but not exactly what would be expected for a second-order peak connected with the peak at $0.18 \,\text{Å}^{-1}$. However, it seems unlikely that a second-order peak would be observed with a principal peak as broad as that at $0.18 \, \text{Å}^{-1}$. While the apparent height was smaller for the curves at 95 °C and 170 °C, for those curves, the scattering from small length scale electron density fluctuations was also much stronger. The cell window material had a broad peak very close to this peak position, and upon subtraction of the empty cell scattering, this feature was substantially reduced in intensity; thus, the strength and position of this feature were strongly dependent upon the precision of the subtraction of the empty cell scattering, leading to more uncertainty in the significance of this feature than for the significance of other features.

Conclusions

The thermal and mechanical properties and morphological features of a depolymerizable graft copolymer thermoplastic have been surveyed. Random incorporation of the comonomers is essential for obtaining a robust material and was confirmed by quantifying the copolymerization kinetics. The findings are consistent with the morphological features seen with SAXS. The PLLA hard segments allow the tuning of the crystallinity and thus of the mechanical properties. Due to the absence of melt-crystallization, the as-molded sample is more amorphous and less ductile than the cold-crystallized material. We believe this easily processible and recyclable thermoplastic will find commercial applications

and offer opportunities for the development of new sustainable materials.

Acknowledgements This work was supported by the University of Akron and the National Science Foundation under Grant No. DMR-2042494. We thank Prof. James M. Eagan for glovebox access and Prof. Kevin Cavicchi for helpful discussion. We acknowledge access to the X-ray scattering facility at the Advanced Materials and Liquid Crystal Institute (AMLCI) at Kent State University, which was financially supported by the National Science Foundation (DMR-2017845), the State of Ohio (The Ohio Department of Higher Education Action Fund), and Kent State University. We thank the Ohio Board of Regents and the National Science Foundation (CHE-0341701 and DMR-0414599) for the funds used to purchase the NMR instrument used in this work.

Compliance with ethical standards

Conflict of interest The authors declare no competing interests.

References

- Duan Y, Thunga M, Schlegel R, Schneider K, Rettler E, Weidisch R, et al. Morphology and deformation mechanisms and tensile properties of tetrafunctional multigraft copolymers. Macromolecules. 2009;42:4155–64.
- Fournier L, Rivera Mirabal DM, Hillmyer MA. Toward sustainable elastomers from the grafting-through polymerization of lactone-containing polyester macromonomers. Macromolecules. 2022;55:1003–14.
- Zhang J, Schneiderman DK, Li T, Hillmyer MA, Bates FS. Design of graft block polymer thermoplastics. Macromolecules. 2016;49:9108–18.
- Vatankhah-Varnosfaderani M, Daniel WFM, Everhart MH, Pandya AA, Liang H, Matyjaszewski K, et al. Mimicking biological stress-strain behaviour with synthetic elastomers. Nature. 2017;549:497–501.
- Vatankhah-Varnosfaderani M, Keith AN, Cong Y, Liang H, Rosenthal M, Sztucki M, et al. Chameleon-like elastomers with molecularly encoded strain-adaptive stiffening and coloration. Science. 2018;359:1509–13.
- Zhang D, Dashtimoghadam E, Fahimipour F, Hu X, Li Q, Bersenev EA, et al. Tissue-adaptive materials with independently regulated modulus and transition temperature. Adv Mater 2020;32:1–11.
- Xiong H, Zhang L, Wu Q, Zhang H, Peng Y, Zhao L, et al. A strain-adaptive, self-healing, breathable and perceptive bottle-brush material inspired by skin. J Mater Chem A. 2020;8:24645–54.
- Dashtimoghadam E, Maw M, Keith AN, Vashahi F, Kempkes V, Gordievskaya YD, et al. Super-soft, firm, and strong elastomers toward replication of tissue viscoelastic response. Mater Horiz 2022;9:3022–30.
- Sveinbjörnsson BR, Weitekamp RA, Miyake GM, Xia Y, Atwater HA, Grubbs RH. Rapid self-assembly of brush block copolymers to photonic crystals. Proc Natl Acad Sci USA. 2012;109:14332–6.
- Guo T, Yu X, Zhao Y, Yuan X, Li J, Ren L. Structure memory photonic crystals prepared by hierarchical self-assembly of semicrystalline bottlebrush block copolymers. Macromolecules. 2020;53:3602–10.
- Zhao TH, Jacucci G, Chen X, Song DP, Vignolini S, Parker RM. Angular-independent photonic pigments via the controlled micellization of amphiphilic bottlebrush block copolymers. Adv Mater 2020;32:1–8.

 Zhang J, Li T, Mannion AM, Schneiderman DK, Hillmyer MA, Bates FS. Tough and sustainable graft block copolymer thermoplastics. ACS Macro Lett. 2016;5:407–12.

- Haugan IN, Maher MJ, Chang AB, Lin TP, Grubbs RH, Hillmyer MA, et al. Consequences of grafting density on the linear viscoelastic behavior of graft polymers. ACS Macro Lett. 2018;7:525–30.
- 14. Leng X, Wei Z, Bian Y, Ren Y, Wang Y, Wang Q, et al. Rheological properties and crystallization behavior of comb-like graft poly(L-lactide): influences of graft length and graft density. RSC Adv. 2016;6:30320–9.
- Hu M, Xia Y, McKenna GB, Kornfield JA, Grubbs RH. Linear rheological response of a series of densely branched brush polymers. Macromolecules. 2011:44:6935

 –43.
- López-Barrón CR, Tsou AH, Younker JM, Norman AI, Schaefer JJ, Hagadorn JR, et al. Microstructure of crystallizable α-olefin molecular bottlebrushes: isotactic and atactic poly(1-octadecene). Macromolecules. 2018:51:872–83.
- Xiang M, Lyu D, Qin Y, Chen R, Liu L, Men Y. Microstructure of bottlebrush poly(n-alkyl methacrylate)s beyond side chain packing. Polymer. 2020;210:123034.
- López-Barrón CR, Hagadorn JR, Mattler SJ, Throckmorton JA. Syndiotactic α-olefin molecular bottlebrushes: crystallization, melting, and hierarchical microstructure. Macromolecules. 2020;53:3778–88.
- Wang Z, Yoon S, Wang J. Breaking the paradox between grafting-through and depolymerization to access recyclable graft polymers. Macromolecules. 2022;55:9249–56.
- Zografos A, Lynd NA, Bates FS, Hillmyer MA. Impact of macromonomer molar mass and feed composition on branch distributions in model graft copolymerizations. ACS Macro Lett. 2021;10:1622–8.

- Zhao C, Wu D, Huang N, Zhao H. Crystallization and thermal properties of PLLA comb polymer. J Polym Sci B Polym Phys. 2008;46:589–98.
- Neugebauer D, Theis M, Pakula T, Wegner G, Matyjaszewski K. Densely heterografted brush macromolecules with crystallizable grafts. Synthesis and bulk properties. Macromolecules. 2006;39:584–93.
- Fischer EW, Sterzel HJ, Wegner G. Investigation of the structure of solution grown crystals of lactide copolymers by means of chemical reactions. Kolloid-Z Z Für Polym. 1973;251:980–90.
- Xia Y, Olsen BD, Kornfield JA, Grubbs RH. Efficient synthesis of narrowly dispersed brush copolymers and study of their assemblies: the importance of side chain arrangement. J Am Chem Soc. 2009:131:18525–32.
- 25. Javni I, Bilić O, Bilić N, Petrović ZS, Eastwood EA, Zhang F, et al. Thermoplastic polyurethanes with controlled morphology based on methylenediphenyldiisocyanate/isosorbide/butanediol hard segments. Polym Int. 2015;64:1607–16.
- Heeley, EL, Billimoria, K, Parsons, N, Figiel, Ł, Keating, EM, Cafolla, CT, et al. In-situ uniaxial drawing of poly-L-lactic acid (PLLA): following the crystalline morphology development using time-resolved SAXS/WAXS. Polymer. 193;2020, https://doi.org/ 10.1016/j.polymer.2020.122353.

Publisher's note Springer Nature remains neutral with regard to jurisdictional claims in published maps and institutional affiliations.

Springer Nature or its licensor (e.g. a society or other partner) holds exclusive rights to this article under a publishing agreement with the author(s) or other rightsholder(s); author self-archiving of the accepted manuscript version of this article is solely governed by the terms of such publishing agreement and applicable law.